



4, 6-Bis[3-(dibenzothiophen-2-yl)phenyl] pyrimidine bipolar host for bright, efficient and low efficiency roll-off phosphorescent organic light-emitting devices



Jing Yu^a, Chunxiu Zang^a, Ziwei Yu^a, Hui Wang^a, Shihao Liu^a, Letian Zhang^a, Wenfa Xie^{a,*}, Hongyu Zhao^{b,**}

^a State Key Laboratory on Integrated Optoelectronics, College of Electronics Science and Engineering, Jilin University, Changchun, 130012, People's Republic of China

^b Beijing Tuocai Optoelectronics Technology Co. Ltd, Beijing, 100086, People's Republic of China

ARTICLE INFO

Article history:

Received 16 June 2016

Received in revised form

26 August 2016

Accepted 3 September 2016

Keywords:

OLED

Bipolar host

Phosphorescent

Roll off

ABSTRACT

A bipolar host 4, 6-Bis[3-(dibenzothiophen-2-yl)phenyl] pyrimidine (DBTPhPm) with small singlet-triplet splitting has been synthesized and confirmed through a series of photophysical and electrochemical properties. Monochromatic phosphorescent organic light-emitting devices (PHOLEDs) based on different hosts [(4,4'-N,N'-dicarbazole) biphenyl, 2,7-bis (diphenylphosphoryl)-9-[4-(N,Ndiphenylamino) phenyl]-9-phenylfluorene, (3,3'-bicarbazole) phenyl and DBTPhPm] and dopants are fabricated. Compared to other hosts, the DBTPhPm-based PHOLEDs exhibited high brightness, high efficiency and low efficiency roll-off. The maximum power efficiency of the DBTPhPm-based red (R), green (G), blue (B), yellow (Y), and orange (O) PHOLEDs are 12.2, 47.2, 17.6, 42.6 and 15.1 lm/W, respectively. The current efficiency roll-off of the R, G, B, Y, and O PHOLEDs are 29.8%, 8.6%, 18.2%, 5.9%, and 22.4% from the maximum current efficiency to the high brightness of 5000 cd/m². The detailed working mechanism of the DBTPhPm-based device is discussed.

© 2016 Elsevier B.V. All rights reserved.

1. Introduction

Phosphorescent organic light-emitting devices (PHOLEDs) have attracted much attention in recent years because their theoretical internal quantum efficiency can be, in principle, three times higher than that of the conventional fluorescent based organic light-emitting devices (OLEDs) through utilizing both singlet and triplet excitons for the light emission, and tremendous efforts have been made in the development of highly efficient PHOLEDs [1–7]. In PHOLEDs, phosphorescent materials are often doped into a suitable host material, which plays an indispensable role in energy transfer and carrier transport, in order to reduce aggregation quenching and triplet-triplet annihilation of guest triplet emitters [8,9]. Therefore, the development of high-performance host materials is extremely essential for PHOLEDs. As an efficient host material, HOMO-LUMO (HOMO: highest occupied molecular

orbital; LUMO: lowest unoccupied molecular orbital) energy band gap (E_g) and triplet energy level (T_1) of the host material must be higher than those of the guest to facilitate energy transfer from the host to guest and to prohibit reverse energy transfer from the guest back to host, and the energy level of the host material must be matched with neighboring layers for both effective carrier injection and carrier confinement [6,10–13]. Besides, a good carrier transport property is expected to restrict the recombination of carriers in the emitting layer (EML) and thus reduce the efficiency roll-off. Traditional host materials usually have good transporting properties for only a single type of carriers. For instance, N, N'-dicarbazolyl-3,5-benzene (mCP) exhibits only good hole-transporting properties, while 3-(4-biphenyl)-4-phenyl-5-(4-tert-butylphenyl)-1,2,4-triazole (TAZ) possesses good electron-transporting abilities [6,11,14,15]. These unbalanced carrier-transporting properties are negative to the turn-on voltage and the efficiency roll-off [11,15–17]. Hence, bipolar host materials that can balance carrier-transporting properties become the focus of attention recently [18–28]. Hsu et al. reported a bipolar host material 2,7-bis (diphenylphosphoryl)-9-[4-(N,Ndiphenylamino) phenyl]-9-

* Corresponding author.

** Corresponding author.

E-mail addresses: xiewf@jlu.edu.cn (W. Xie), zhy_china@126.com (H. Zhao).

phenylfluorene (POAPF), and the corresponding blue monochromatic OLEDs own a rather low turn-on voltage of 2.5 V due to the balance of carriers in the EML [24]. Zheng et al. applied a series of new synthesis host materials to blue monochromatic OLEDs, and obtained a low voltage of 2.6 V and a gentle efficiency roll-off. The device using 9,9-bis(9-methylcarbazol-3-yl)-4,5-diazafluorene (MCAF) as the host has a maximum current efficiency (CE) of 32.2 cd/A and a maximum power efficiency (PE) of 31.3 lm/W, and still keep a high CE of 27.6 cd/A and a high PE of 14.5 lm/W at the brightness of 10000 cd/m² [29]. Furthermore, Son et al. achieved bipolar host materials 4-(*N*-a-carbolinyl)-4'-(*N*-carbazolyl) triphenylamine (ADCTA), 4,4'-di(*N*-a-carbolinyl)-4''-(*N*-carbazolyl) triphenylamine (DACTA) and 4,4',4''-(*N*-acarbolinyl) triphenylamine (TATA) with the nature of small singlet-triplet energy gap (ΔE_{S-T} : the difference between singlet and triplet energy levels) so that the dopant may avoid being deep trap sites due to the small singlet to triplet splitting energy (0.4 eV) [30,31].

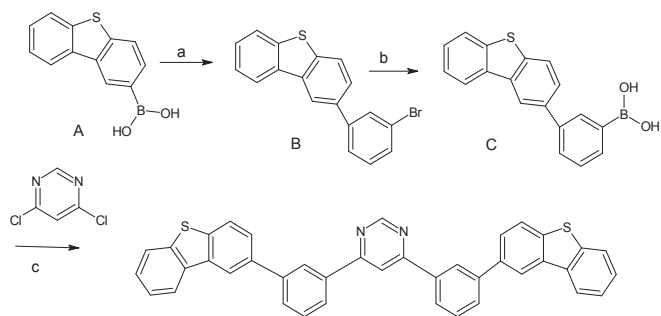
In this paper, a bipolar host material 4,6-Bis[3-(dibenzothiophen-2-yl)phenyl] pyrimidine (DBTPhPm) is reported and a series of low-voltage, highly efficient, and low efficiency roll-off DBTPhPm-based PHOLEDs are designed. Iridium (III) Bis [1-(3,5-dimethylphenyl)-7-methylisoquinoline] (acetylacetonate) [Ir(pmi-q)₂(acac)], tris(2-phenylpyridine) iridium [Ir(ppy)₃], [(bis[2-(4,6-difluorophenyl)pyridyl-N,C^{2'}] iridium (III) [Firpic], Iridium(III)bis(2-methyldibenzo-[f,h] quinoxaline) (acetylacetonate) [Ir(MD-Q)₂(acac)] and Iridium(III) bis(4-phenylthieno [3,2-c] pyridinato-N,C^{2'}) acetylacetonate [PO-01] are used as the red, green, blue, orange, and yellow dopants. For comparison, device using (4,4'-*N,N'*-dicarbazole) biphenyl (CBP), POAPF and (3,3'-bicarbazole) phenyl (BCZph) [32] as host were also fabricated. The results indicated that DBTPhPm is an efficient host for most common phosphorescent dopants.

2. Experimental

UV–visible absorption and photoluminescence (PL) studies at room temperature were carried out using U3010 spectrometer (Hitachi, Japan) and F-7000 FL spectrophotometer, respectively. The phosphorescence spectrum was recorded from the delayed emission of DBTPhPm at 77 K. The cyclic voltammogram (CV) experiments were performed using a BAS 100 W instrument at room temperature in CH₂Cl₂ solutions at a scan rate of 100 mV/s. All devices were fabricated on glasses substrates covered by conducting indium tin oxide (ITO). The substrates were cleaned in Decon 90 and deionized water, dried in the oven and then treated in plasma for about 5 min. Finally organic layers and cathode materials were sequentially deposited on the substrates without breaking vacuum ($\sim 5.0 \times 10^{-4}$ Pa). A shadow mask was used to define the cathode and to make four 10 mm² devices on each substrate. Current–Voltage–Luminance (I–V–L) characteristics of unpackaged devices were measured with a Keithley 2400 Source Meter and a Minolta Luminance Meter LS-110. The spectra of the devices were measured with Ocean Optics Maya 2000-PRO spectrometer.

3. Results and discussion

Scheme 1 depicts the synthetic route and structure of the new host material DBTPhPm. Dibenzothiophene-2-boronic acid was purchased from Bepfarm Chemical (China). The boronic acid C was synthesized according to literature [33]. Other reactants or reagents were used as received. 10 g (67 mmol) 4,6-dichloropyrimidine, 60 g (20 mmol) 3-(dibenzothiophen-2-yl) phenylboronic acid, 80 g (70 mmol) K₂CO₃, 500 ml toluene and 200 ml H₂O were put in a 1 L recovery flask. While the pressure was reduced, the mixture was



Scheme 1. Synthetic routes to DBTPhPm. (a) toluene, H₂O, K₂CO₃, PdCl₂(PPh₃)₂; (b) THF, -78 °C, n-BuLi, B(OPr)₃; (c) toluene, H₂O, K₂CO₃, PdCl₂(PPh₃)₂.

stirred to be degassed. Then 0.5 g PdCl₂(PPh₃)₂ was added in this mixture and the atmosphere was replaced with N₂. The mixture was stirred while reaction container was heated. After heating, water was added to the mixture, and the mixture was filtered to give residue. The obtained solid was washed with dichloromethane and methanol. The obtained solid was recrystallized from toluene to give 25 g white solid (yield 63%). ¹H NMR(CDCl₃, 400 MHz): 7.41–7.51 (m, 4H), 7.58–7.62 (m, 4H), 7.68–7.79 (m, 4H), 8.73 (dt, 2H), 8.18–8.27 (m, 7H), 8.54 (t, 2H), 9.39 (d, 1H). MODI-TOF: 596.76. Anal. calcd for C₄₀H₂₄N₂S₂ (%): C 80.51, H 4.05, N 4.69, S 10.75; Found: C 80.50, H 4.05, N 4.71, S 10.74.

DBTPhPm has a simple molecular structure that having two dibenzothiophene and one pyrimidine moiety. Pyrimidine core structure was designed as the electron transport type core structure with high triplet energy and high rigidity for high glass transition temperature ($T_g = 268.9$ °C). The T_g of DBTPhPm is much higher than that of the CBP(62 °C) [34], POAPF(129 °C) [24] and BCZph(100 °C) [35]. The high T_g would be benefited to the stability of the devices. The dibenzothiophene unit withdraws electron due to S atom with high electronegativity. The ultraviolet–visible (UV–vis) absorption, PL emission and low-temperature photoluminescence (LTPL) emission spectra of DBTPhPm in CH₂Cl₂ solution (1×10^{-5} M) are measured, and Fig. 1 shows the characteristics with an inset figure of the chemical structure of DBTPhPm. Absorption peaks at 336 nm can be attributed to π - π^* transitions of the dibenzothiophene chromophore and π - π^* and n - π^* transitions of central aryls, respectively. The optical energy band gap (E_g) of DBTPhPm is calculated to be 3.69 eV from the onset of the absorption spectrum (336 nm) according to the UV–vis absorption curve. The fluorescence emission peak of DBTPhPm is

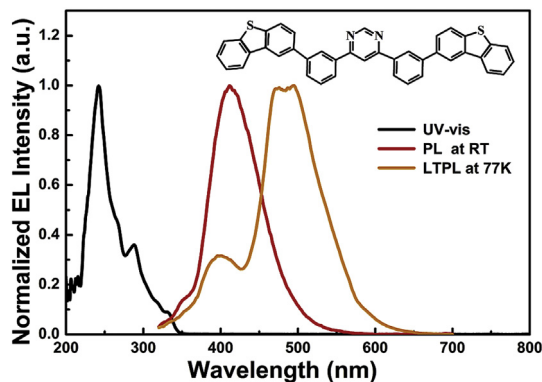


Fig. 1. The UV–vis absorption, photoluminescence (PL) emission (at RT) and low-temperature photoluminescence (LTPL) emission (at 77 K) spectra of DBTPhPm in CH₂Cl₂ solution (1×10^{-5} M).

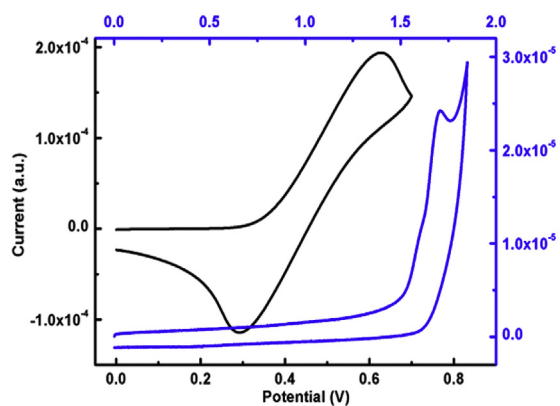


Fig. 2. Cyclic voltammogram of DBTPhPm.

411 nm and its single state (S_1) is estimated to be 3.02 eV accordingly. The phosphorescence spectrum is obtained from the delayed emission of DBTPhPm at 77 K and the triplet energy (T_1) is

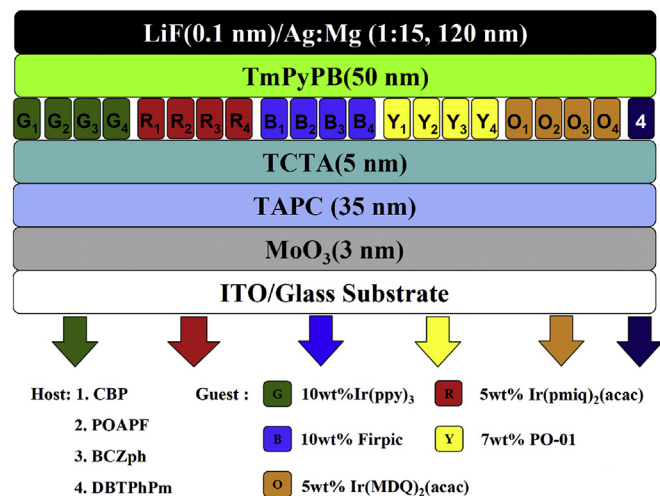


Fig. 4. The structures of red (R), green (G), blue (B), yellow (Y), and orange (O) PHOLEDs with different hosts and dopants. (For interpretation of the references to colour in this figure legend, the reader is referred to the web version of this article.)

Table 1

The physical properties of DBTPhPm.

Absorption: λ_{abs} (nm) ^a	λ_{fluor} (nm) ^a	λ_{phos} (nm) ^b	HOMO (eV) ^c	LUMO (eV) ^d	E_g (eV) ^e	S_1 (eV)	T_1 (eV)	E_{S-T} (eV) ^f
288, 336	411	471	-5.88	-2.19	3.69	3.02	2.63	0.39

^a Measured in CH_2Cl_2 solution (10^{-5} M) at room temperature (RT).

^b Measured in CH_2Cl_2 solution (10^{-5} M) at 77 K.

^c HOMO was estimated by CV.

^d LUMO was calculated from the difference of HOMO and E_g .

^e The optical energy band gap was calculated from the equation $E_g = hc/\lambda = 1240/\lambda$, where λ is the wavelength of the onset of the absorption spectrum.

^f Singlet-triplet energy gap: the difference between singlet and triplet energy levels.

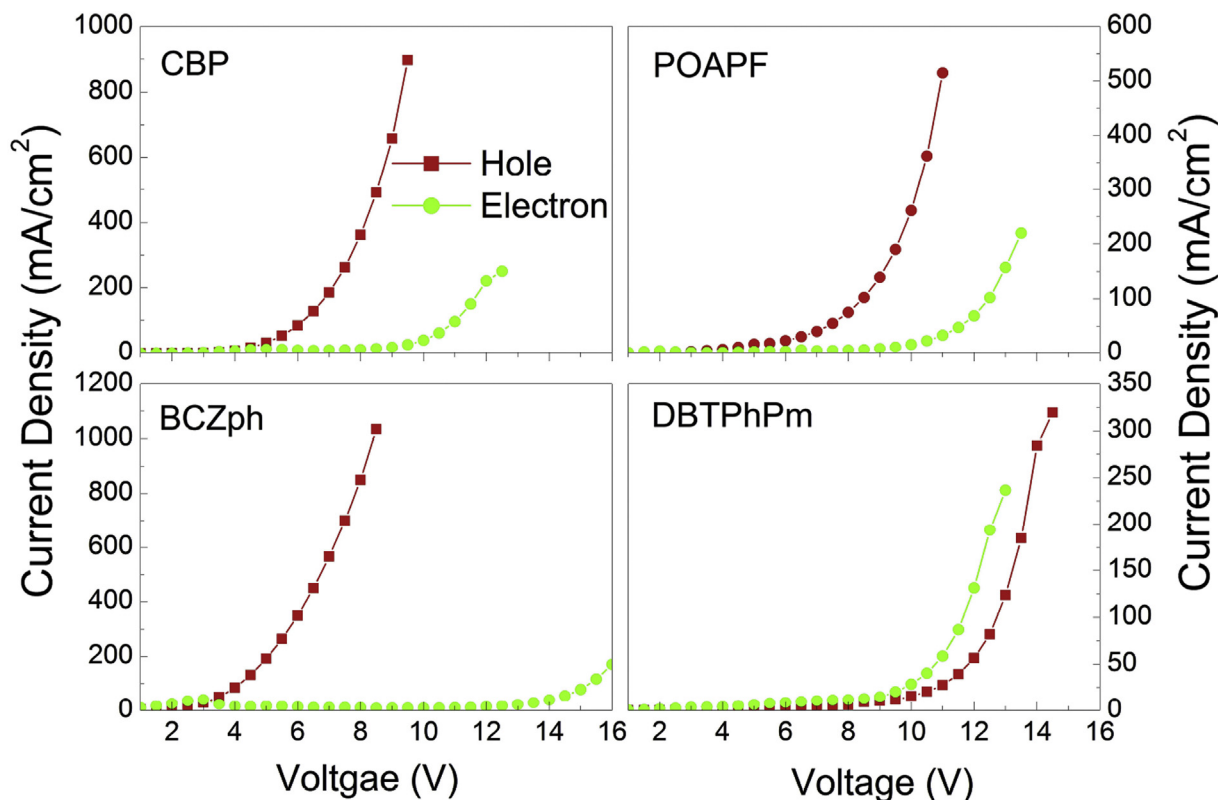


Fig. 3. Current density-voltage characteristics of the hole-only and electron-only devices with different hosts.

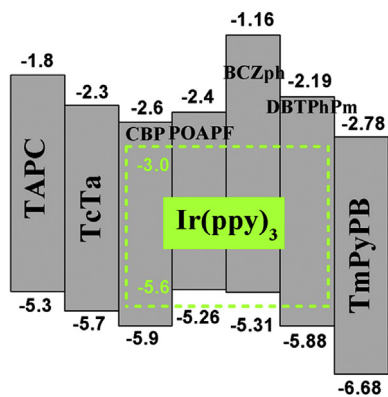


Fig. 5. The energy level diagrams of devices G_1 – G_4 .

estimated to be 2.63 eV (471 nm) which results in a small ΔE_{S-T} (0.39 eV) of DBTPhPm. The electrochemical properties of DBTPhPm sample are investigated with cyclic voltammetric (CV). The CV curve of DBTPhPm is shown in Fig. 2. According to the onset potential of its oxidation process, the HOMO energy level of DBTPhPm is estimated to be approximately -5.88 eV, and the corresponding LUMO energy level is calculated to be -2.19 eV, referring to the HOMO and absorption spectra [36]. All photophysical data and electrochemical properties of DBTPhPm are summarized in Table 1.

The electron-/hole-transporting characters of the hosts are investigated with the fabrication of the hole-only and electron-only devices. The hole-only device has the structure of ITO/MoO₃

(3 nm)/TAPC: MoO₃ (6:1 by weight, 20 nm)/TAPC (20 nm)/TCTA (5 nm)/host (20 nm)/TAPC (40 nm)/MoO₃ (3 nm)/Ag (120 nm) [where TAPC is 1,1-Bis[(di-4-toly-lamino)phenyl]cyclohexane, TCTA is 4,4',4''-tris (Ncarbazolyl) triphenylamine], while the electron-only device has the structure of ITO/LiF (0.5 nm)/1,3,5-tris (*m*-pyrid-3-yl-phenyl) benzene (TmPyPB: 60 nm)/host (20 nm)/4,7-diphenyl-1,10-phenanthroline (Bphen: 40 nm)/Ag (120 nm). It is supposed that only single carriers are injected and transported in the devices due to the work function of MoO₃ (or LiF) being high (or low) enough to block electron (or hole) injection. The current density of the single-carrier devices are plotted against voltage in Fig. 3. As can be seen, the four hosts have the carrier transporting ability of both holes and electrons. CBP, POAPF and BCZph perform better hole-transport properties and there is a huge difference between the hole- and electron-transport properties for BCZph. However, DBTPhPm performs balanced hole- and electron-transport properties.

To investigate the DBTPhPm as host in PHOLEDs, PHOLEDs with the structure of ITO/MoO₃ (3 nm)/TAPC (35 nm)/TCTA (5 nm)/emitting layer (EML: 20 nm)/TmPyPB (50 nm)/LiF (0.5 nm)/Mg:Ag (15:1 by weight, 120 nm) as depicted in Fig. 4 were fabricated. The EML was host doped with different guests. The hosts were CBP, POAPF, BCzPh, and DBTPhPm, the guests were Ir(ppy)₃ (green), Ir(pmq)₂(acac) (red), Firpic (blue), PO-01 (yellow), and Ir(MD-Q)₂(acac) (orange), respectively. As examples, the green PHOLEDs are demonstrated in detail, and the corresponding energy level diagrams of green PHOLEDs are shown in Fig. 5. TAPC with LUMO energy level of 1.8 eV (LUMO: 2.6 eV for CBP, 2.4 eV for POAPF, 1.16 eV for BCZph, 2.19 eV for DBTPhPm) and high triplet energy level (T_1) of 2.9 eV (T_1 : 2.56 eV for CBP, 2.75 eV for POAPF, 2.87 eV

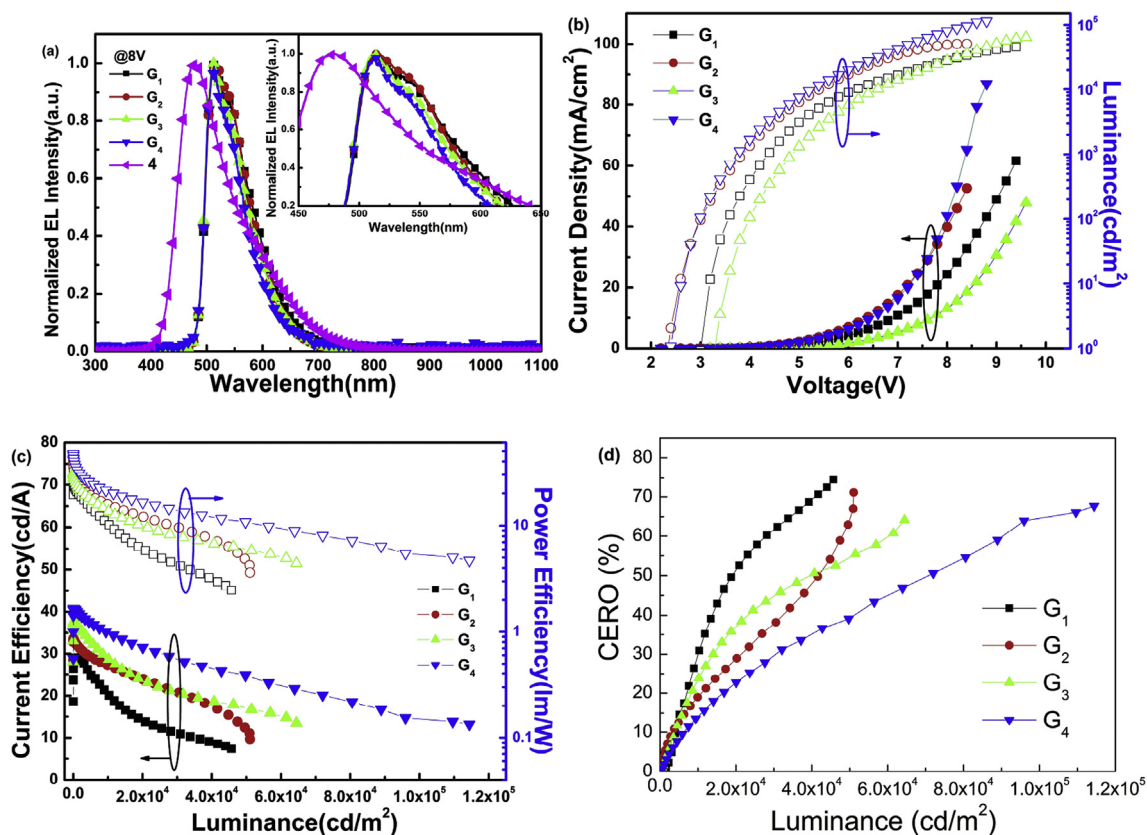


Fig. 6. Performances of devices G_1 – G_4 . (a) Normalized EL spectra at 8 V. (b) Current density–voltage–luminance characteristics. (c) Current efficiency–luminance–power efficiency characteristics. (d) Current efficiency roll-off characteristics.

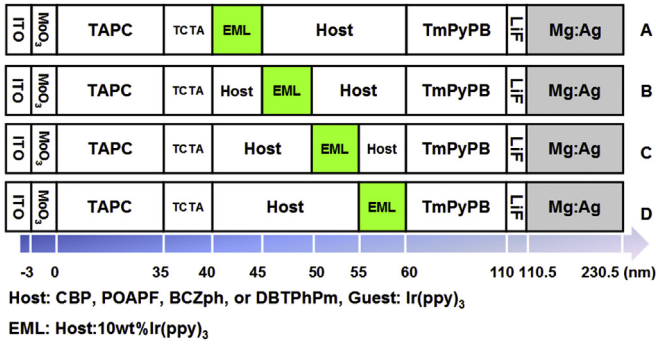


Fig. 7. The device structure of the green PHOLEDs with moving EML. (For interpretation of the references to colour in this figure legend, the reader is referred to the web version of this article.)

for BCZph, 2.63 eV for DBTPhPm) is used as hole transport layer (HTL), while TmPyPB with HOMO energy level of 6.68 eV (HOMO: 5.9 eV for CBP, 5.26 eV for POAPF, 5.31 eV for BCZph, 5.88 eV for DBTPhPm) and triplet energy level of 2.78 eV is used as electron transport layer (ETL) in the devices for the effective confinement of carriers and/or excitons within the EML [37].

The electrical properties of the green devices are shown in Fig. 6. Fig. 6(a) depicts the normalized electroluminescence (EL) spectra of green devices and undoped DBTPhPm device (device 4 as shown in Fig. 4) at 8 V. Devices G₁–G₄ show the EL emission peak at 512 nm with CIE color coordinate of about (0.32, 0.60) that is originate from Ir(ppy)₃. No extra emission from the host and/or the adjacent carrier transporting layers except the green emission indicates that the confinement of carriers is effective and the energy transfer from host to guest is complete. Fig. 6 (b) shows the current density-voltage-luminance (J-V-L) curves of device G₁–G₄. The turn-on voltage (driving voltage @ 1 cd/m²) of G₂ and G₄ is 2.3 V and

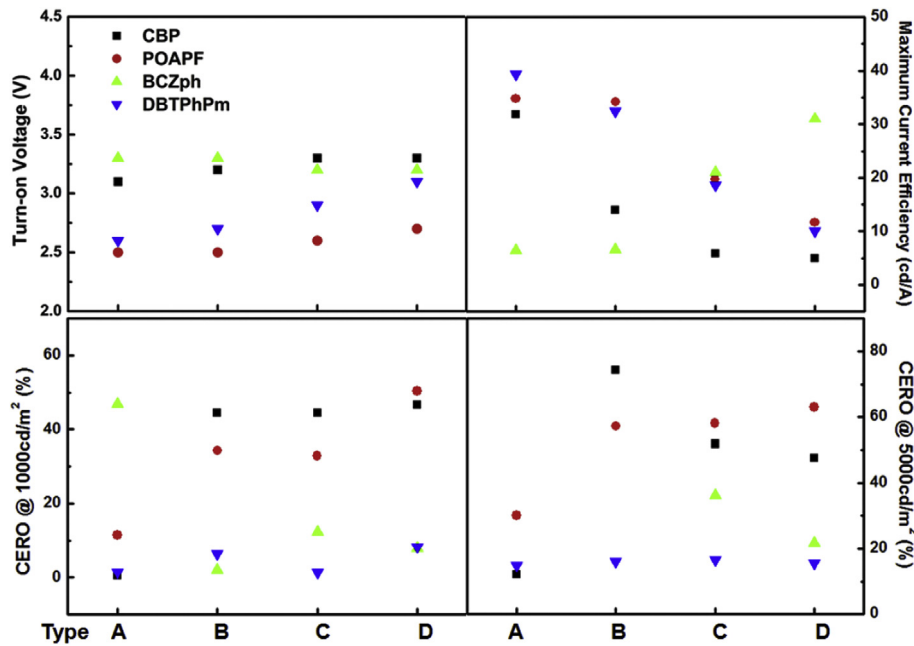


Fig. 8. Turn-on voltage, maximum current efficiency, and current efficiency roll-off characteristics of the green PHOLEDs with moving EML. (For interpretation of the references to colour in this figure legend, the reader is referred to the web version of this article.)

Table 2
Characteristics based on devices.

Device	V _{on} (V)	L _{max} (cd/m ²)	η _{c,max} , η _{c,1000} , η _{c,5000} (cd/A)	η _{p,max} , η _{p,1000} , η _{p,5000} (lm/W)	CERO (%) ^{a,b}	PERO (%) ^{a,b}
R ₁	3.1	20240	8.6, 5.9, 4.5	8.5, 3.1, 1.8	31.4, 47.7	63.5, 78.8
R ₂	2.5	9393	8.1, 5.7, 3.8	10.5, 3.6, 1.6	29.6, 53.1	65.7, 84.8
R ₃	3.3	6758	6.8, 3.5, 1.5	6.2, 1.7, 0.5	48.5, 77.9	72.6, 91.9
R ₄	2.5	19650	10.4, 9.5, 7.3	12.2, 6.8, 3.8	8.7, 29.8	44.3, 68.9
B ₁	3.1	10050	22.7, 9.5, 4.3	23.7, 6.1, 1.9	58.1, 81.1	74.3, 92
B ₂	2.5	5969	19.9, 17.4, 6.8	21.6, 13, 3.5	12.6, 65.8	39.8, 83.8
B ₃	3.1	11570	23.8, 16.1, 6.8	22.1, 10.1, 3.1	32.4, 71.4	54.3, 86
B ₄	2.7	18040	17.6, 17.2, 14.4	17.6, 12.8, 8.4	2.3, 18.2	27.3, 52.3
Y ₁	2.9	76850	34.5, 34.5, 32.3	31.1, 25.8, 19.6	/, 6.4	17, 37
Y ₂	2.3	40420	33.9, 31.7, 27.8	46.9, 27.7, 19.1	6.5, 18	41, 59.3
Y ₃	3.1	26740	33.2, 32, 24	29.8, 22.9, 14	4, 27.7	23.2, 53
Y ₄	2.5	97150	39.3, 39.1, 37	42.6, 33, 25.3	0.5, 5.9	22.5, 40.6
O ₁	3.3	15070	15.6, 10.8, 5.6	14.9, 6.5, 2.6	30.8, 64.1	56.4, 82.6
O ₂	2.7	15090	12.2, 9.8, 6.4	13.4, 6.6, 3.3	19.7, 47.5	50.7, 75.4
O ₃	3	12170	16.8, 13.4, 4.6	15.1, 8.5, 2.1	20.2, 72.6	43.7, 86.1
O ₄	2.7	39290	14.7, 13.4, 11.4	15.1, 9.3, 6	8.8, 22.4	38.4, 60.3

^a Values collected from the maximum to the luminance of 1000 cd/m².

^b Values collected from the maximum to the luminance of 5000 cd/m².

2.4 V, while that of G_1 and G_3 is high to 3 V and 3.3 V, respectively. The maximum brightness of devices G_1 – G_4 is 45700, 51040, 64440 and 114400 cd/m^2 , respectively. Fig. 6 (c) exhibits the efficiency-luminance characteristics of devices G_1 – G_4 . The maximum current efficiency (CE) of device G_4 is 40.7 cd/A , and as a result of the low driving voltage, the maximum power efficiency (PE) is 47.2 lm/W , which are much higher than G_1 – G_3 (CE: 29.1 cd/A , 33.6 cd/A , 37.6 cd/A , PE: 24.4 lm/W , 42.9 lm/W , 31.2 lm/W). At the high brightness of 1000 cd/m^2 , the CE of G_4 maintains 40.3 cd/A , and the corresponding PE is 35.2 lm/W . Even at the brightness of 10000 cd/m^2 , the CE and PE can still reach 35.1 cd/A and 20.8 lm/W . The CE roll-off (CERO) of devices G_1 – G_4 are shown in Fig. 6 (d). As can be seen, the efficiency roll-off of device G_4 is much lower than others at high brightness. For example, at brightness of 20000 cd/m^2 , the CERO is 22.8% for device G_4 , which are 51.4%, 28.6%, and 37.0% for device G_1 – G_3 . Therefore, it can be concluded that device G_4 has an overwhelming superiority on efficiency and efficiency roll-off comparing with device G_1 – G_3 .

To investigate the working mechanism of the green PHOLEDs, four type devices with structure as depicted in Fig. 7 were fabricated. In the devices with same host, the EML was moved from anode side to cathode side. The detailed performances of the devices are shown in Fig. 8. The maximum current efficiencies of BCZph-based devices are decreased when the EML is moved from cathode side to anode side, and the maximum current efficiencies of other devices are decreased when the EML is moved from anode side to cathode side. Besides, the EL spectra of the Type A, B and C devices with BCZph host show the emission from BCZph, while no host emission is observed in other devices. From Fig 6 (b), we also can see that the maximum efficiency decrease with the EML moving is obviously. Besides, the CERO of the devices based on DBTPhPm host is independent on the location of the EML, while the CERO of other devices is dependent on the location of the EML. The results indicated that the recombination zone of device G_3 (host: BCZph) is closed to EML/ETL interface due to the high LUMO energy barrier between TmPyPB and BCZph and excellent hole-transport properties of BCZph, while it would be the entire EML for device G_1 (host: CBP), G_2 (host: POAPF) and G_4 (host: DBTPhPm). However, more excitons are generated at HTL/EML interface in device G_1 , which are generated at both the HTL/EML and EML/ETL interfaces in device G_2 and G_4 . Thus, the CERO of device G_2 and G_4 would be lower in principle. In fact, the efficiency roll-off of device G_2 and G_4 is relative low. According to the results, we think bipolar transporting property of DBTPhPm and energy level matching to the adjacent HTL and ETL are not all of the reason for extremely low efficiency roll-off in DBTPhPm-based device. Another important reason is the small ΔE_{S-T} (0.39 eV) of DBTPhPm, which is about 0.51 [38], 0.49 [24] and 0.43 eV [35] for CBP, POAPF and BCzPh, which avoid the dopants being deep trap sites. Moreover, the red, blue, yellow and orange monochromatic OLEDs based on DBTPhPm host are also show excellent performances compare other devices with CBP, POAPF, or BCZph host and the details are listed in Table 2.

4. Conclusions

In summary, a new bipolar host material DBTPhPm has been synthesized and a series of photophysical and electrochemical properties of DBTPhPm has been confirmed. A systematic research on red, green, blue, yellow and orange monochromatic organic light-emitting devices based on different hosts is demonstrated. The results show that DBTPhPm is an efficient host material for most common phosphorescent dopants. The DBTPhPm-based device exhibits high brightness, low turn-on voltage, high efficiency

and low efficiency roll-off. It could be attributed to the balanced bipolar transporting properties and small singlet-triplet energy gap of DBTPhPm.

Acknowledgements

This work was supported by the National Natural Science Foundation of China (Grant Nos. 61474054, 61475060, 61177026).

References

- [1] M.A. Baldo, D.F. O'Brien, Y. You, A. Shoustikov, S. Sibley, M.E. Thompson, S.R. Forrest, *Nature* 395 (1998) 151.
- [2] D.F. O'Brien, M.A. Baldo, M.E. Thompson, S.R. Forrest, *Appl. Phys. Lett.* 74 (1999) 442.
- [3] M.A. Baldo, S. Lamansky, P.E. Burrows, M.E. Thompson, S.R. Forrest, *Appl. Phys. Lett.* 75 (1999) 4.
- [4] M.A. Baldo, M.E. Thompson, S.R. Forrest, *Nature* 403 (2000) 750.
- [5] R.C. Kwong, S. Lamansky, M.E. Thompson, *Adv. Mater.* 12 (2000) 1134.
- [6] C. Adachi, M.A. Baldo, M.E. Thompson, S.R. Forrest, *J. Appl. Phys.* 90 (2001) 5048.
- [7] T. Tsuzuki, N. Shirasawa, T. Suzuki, S. Tokito, *Adv. Mater.* 15 (2003) 1455.
- [8] M.A. Baldo, S.R. Forrest, *Phys. Rev. B* 62 (2000) 10958.
- [9] M.A. Baldo, C. Adachi, S.R. Forrest, *Phys. Rev. B* 62 (2000) 10967.
- [10] D.S. Leem, S.O. Jung, S.O. Kim, J.W. Park, J.W. Kim, Y.S. Park, Y.H. Kim, S.K. Kwon, J.J. Kim, *J. Mater. Chem.* 19 (2009) 8824.
- [11] R.J. Holmes, S.R. Forrest, Y.J. Tung, R.C. Kwong, J.J. Brown, S. Garon, M.E. Thompson, *Appl. Phys. Lett.* 82 (2003) 2422.
- [12] S.J. Yeh, M.F. Wu, C.T. Chen, Y.H. Song, Y. Chi, M.H. Ho, S.F. Hsu, C.H. Chen, *Adv. Mater.* 17 (2005) 285.
- [13] X.F. Ren, J. Li, R.J. Holmes, P.I. Djurovich, S.R. Forrest, M.E. Thompson, *Chem. Mater.* 16 (2004) 4743.
- [14] T. Thoms, S. Okada, J.P. Chen, M. Furugori, *Thin Solid Films* 436 (2003) 264.
- [15] C. Adachi, M.A. Baldo, S.R. Forrest, M.E. Thompson, *Appl. Phys. Lett.* 77 (2000) 904.
- [16] N.J. Lundin, A.G. Blackman, K.C. Gordon, D.L. Officer, *Angew. Chem. Int. Ed.* 45 (2006) 2582.
- [17] C.T. Chen, Y. Wei, J.S. Lin, M. Moturu, W.S. Chao, Y.T. Tao, C.H. Chien, *J. Am. Chem. Soc.* 128 (2006) 10992.
- [18] X.Y. Cai, A.B. Padmaperuma, L.S. Sapochak, P.A. Vecchi, P.E. Burrows, *Appl. Phys. Lett.* 92 (2008) 083308.
- [19] Y.T. Tao, Q. Wang, C.L. Yang, Z.Q. Zhang, T.T. Zou, J.G. Qin, D.G. Ma, *Angew. Chem. Int. Ed.* 47 (2008) 8104.
- [20] Z.Y. Ge, T. Hayakawa, S. Ando, M. Ueda, T. Akiike, H. Miyamoto, T. Kajita, M.A. Kakimoto, *Adv. Funct. Mater.* 18 (2008) 584.
- [21] M.Y. Lai, C.H. Chen, W.S. Huang, J.T. Lin, T.H. Ke, L.Y. Chen, M.H. Tsai, C.C. Wu, *Angew. Chem. Int. Ed.* 47 (2008) 581.
- [22] S.J. Su, H. Sasabe, T. Takeda, J.J. Kido, *J. Chem. Mater.* 20 (2008) 1691.
- [23] Z.Q. Gao, M. Luo, X.H. Sun, H.L. Tam, M.S. Wong, B.X. Mi, P.F. Xia, K.W. Cheah, C.H. Chen, *Adv. Mater.* 21 (2009) 688.
- [24] F.M. Hsu, C.H. Chien, C.F. Shu, C.H. Lai, C.C. Hsieh, K.W. Wang, P.T. Chou, *Adv. Funct. Mater.* 19 (2009) 2834.
- [25] S.O. Jeon, K.S. Yook, C.W. Joo, J.Y. Lee, *Adv. Funct. Mater.* 19 (2009) 3644.
- [26] H.H. Chou, C.H. Cheng, *Adv. Mater.* 22 (2010) 2468.
- [27] Y.T. Tao, C.L. Yang, J.G. Qin, *Chem. Soc. Rev.* 40 (2011) 2943.
- [28] S.L. Gong, Q. Fu, Q. Wang, C.L. Yang, C. Zhong, J.G. Qin, D.G. Ma, *Adv. Mater.* 23 (2011) 4956.
- [29] C.J. Zheng, J. Ye, M.F. Lo, M.K. Fung, X.M. Ou, X.H. Zhang, C.S. Lee, *Chem. Mater.* 24 (2012) 643.
- [30] Y.H. Son, Y.J. Kim, M.J. Park, H.Y. Oh, J.S. Park, J.H. Yang, M.C. Suh, J.H. Kwon, *J. Mater. Chem. C* 1 (2013) 5008.
- [31] K. Brunner, A.V. Dijken, H. Borner, J.J.A.M. Bastiaansen, N.M.M. Kiggen, B.M.W. Langeveld, *J. Am. Chem. Soc.* 126 (2004) 6035.
- [32] H. Sasabe, N. Toyota, H. Nakanishi, T. Ishizaka, Y.J. Pu, J.J. Kido, *Adv. Mater.* 24 (2012) 3212.
- [33] S.C. Dong, Y. Liu, Q. Li, L.S. Cui, H. Chen, Z.Q. Jiang, L.S. Liao, *J. Mater. Chem. C* 1 (2013) 6575.
- [34] M.-H. Tsai, Y.-H. Hong, C.-H. Chang, H.-C. Su, C.-C. Wu, A. Matoliuskyte, J. Simokaitiene, S. Grigalevicius, J.V. Grazulevicius, C.-P. Hsu, *Adv. Mater.* 19 (2007) 862.
- [35] L.S. Cui, Y. Liu, X.D. Yuan, Q. Li, Z.Q. Jiang, L.S. Liao, *J. Mater. Chem. C* 1 (2013) 8177.
- [36] J.Q. Ding, B. Wang, Z.Y. Yue, B. Yao, Z.Y. Xie, Y.X. Cheng, L.X. Wang, X.B. Jing, F.S. Wang, *Angew. Chem. Int. Ed.* 48 (2009) 6664.
- [37] M.G. Shin, K. Thangaraju, S. Kim, J.W. Park, Y.H. Kim, S.K. Kwon, *Org. Electron.* 12 (2011) 785.
- [38] S. Reineke, G. Schwartz, K. Walzer, K. Leo, *Phys. Status. Solidi. RRL* 3 (2009) 67.